Use of Biophysical Characterization in Preformulation Development of a Heavy-Chain Fragment of Botulinum Serotype B: Evaluation of Suitable Purification Process Conditions

Frank K. Bedu-Addo,[1,3] Catharine Johnson,[1,4] Shanthini Jeyarajah,[1] Ian Henderson,[2] and Siddharth J. Advant[1,5]

Received August 7, 2003; accepted April 28, 2004

Purpose. The purpose of this study was to investigate the physicochemical and structural characteristics of recombinant botulinum serotype B (rBoNTB(Hc)) under various conditions and to use the information in evaluating suitable purification process conditions.
Methods. The solubility of rBoNTB(Hc) was evaluated at pH 4, 5, 6 7.5, 8, and 9. Secondary structure was evaluated using circular dichroism, and conformational stability was monitored using high-sensitivity differential scanning calorimetry. Hydrophobic interaction chromatography, size exclusion chromatography-high performance liquid chromatography (SEC-HPLC), sodium dodecyl sulfate-poly acrylamide gel electrophoresis (SDS-PAGE), peptide mapping, and UV spectroscopy were used to monitor stability under the various conditions.
Results. The secondary structure of rBoNTB(Hc) consists predominantly of β-sheets. Solubility of rBoNTB(Hc) was lowest at its pI and highest at low and high pH. In the presence of NaCl, however, solubility decreased with increase in pH. Conformational and chemical stability are improved below pH 7.5. In the presence of 150 mM NaCl at high pH, conformational and chemical stability of rBoNTB(Hc) are further decreased. The study suggests that the purification process should minimize exposure of rBoNTB(Hc) to high pH and salt conditions.
Conclusions. Optimal stability of rBoNTB(Hc) is achieved at low pH. The biophysical and analytical studies provide us with an understanding of rBoNTB(Hc) stability behavior in solution and assists in developing efficient purification conditions.

KEY WORDS: botulinum neurotoxin; circular dichroism; differential scanning calorimetry; proteins; purification.

INTRODUCTION

Seven serologically distinct forms of the botulinum neurotoxin (A–G) are produced by the gram-positive bacteria *Clostridium botulinum*. The seven serotypes have similar structure but differing antigenic specificity (1,2). These neurotoxins are among the most poisonous presently known, with human LD_{50} values in the range 0.1–1.0 ng/kg (3). Food poisoning is the most common source of botulism with the result being a fatal paralysis of the respiratory muscles (4,5). The use of toxins such as the botulinum neurotoxins in biological warfare (6) have increased the need for a safe and efficacious vaccine against all seven serotypes.

Botulinum neurotoxins are all produced as single polypeptide chains of approximately 150 kDa that are cleaved by tissue proteinases into a heavy chain of 100 kDa and a light chain of 50 kDa linked by a single disulfide bond (3,7,8). It is known that the C-terminal portion of the heavy chain binds the toxin to neuron receptors (9,10), whereas the N-terminal portion controls internalization of the light chain, which targets nerve cells (11). Although the complete toxin is required for toxicity to occur, the heavy-chain fragments alone have been found to be nontoxic and antigenic (12). Studies performed with animals have shown the ability of the heavy-chain fragment to elicit a protective immune response when challenged with native botulism toxin (13–15). Investigations are currently ongoing to develop a multivalent vaccine against all seven serotypes of botulism using the heavy-chain fragments of the botulinum neurotoxin (16–20).

Secondary structure of the botulinum neurotoxins has been found to be dependent on pH (2); however, similar studies have not been performed with the recombinant heavy-chain fragments that are being used to develop the multivalent vaccines. These antigens are all approximately 50 kDa with pI ranging from pH 5 to pH 9. This paper describes structural and chemical characterization of recombinant botulinum serotype B (BoNTB(H_c)) as a function of pH and ionic strength, with the goal of using the information to evaluate efficient purification conditions for BoNTB(H_c).

Conformational analysis is used to understand the stability of BoNTB(H_c) under the various conditions. In developing a purification process, physical and chemical stability of the protein are usually considered while ignoring the effects of potential processing conditions on the conformation of the protein. Protein conformation in most cases will influence both biological activity and physical stability and could also play a very significant role in determining final processing yields. Conformational analysis has however been used by a few groups in formulation development (21–23).

MATERIALS AND METHODS

Synthesis and Purification

The heavy-chain fragment of the botulinum serotype B (BoNTB(Hc)) used in the study was produced at Diosynth RTP, Inc. (Cary, NC, USA) prior to optimization of the process. This protein has a molecular weight of approximately 50 kDa and a pI between 6.5 and 7.5.

Chemicals

All chemicals used were USP grade, obtained from J. T. Baker (Phillipsburg, NJ, USA).

Dialysis

After production, rBoNTB(Hc) was diafiltered to a concentration of 1.0 mg/ml (by UV_{280}) in 25 mM sodium acetate buffer, pH 5.0. Dialysis was performed for 18 h using Slide-

[1] Diosynth RTP, Inc., Cary, North Carolina 27513, USA.
[2] Dynport Vaccine Company, LLC, Frederick, Maryland 21702, USA.
[3] Present address: KBI BIOPHARMA, Inc., Durham, North Carolina 27704, USA.
[4] Present address: Boehringer Ingelheim Pharmaceuticals, Inc., Ridgefield, Connecticut 06877, USA.
[5] To whom correspondence should be addressed. (e-mail: sid.advant@diosynth-rtp.com)

A-Lyzer cassettes (3,500 molecular weight cutoff), obtained from Pierce (Rockford, IL, USA) into buffers of selected pH and NaCl concentration. NaCl concentration of 150 mM was selected based on potential purification conditions. (See key on Fig. 6 for buffer compositions.)

Circular Dichroism

Circular dichroism (CD) studies were performed to determine the secondary structure of the protein and to determine structural changes of the protein under various conditions. Ellipticity was monitored at 216- and 230-nm wavelength. An OLIS RSM 1000 spectrometer (Bogart, GA) was used. Scanning was performed at ambient temperature from 260 to 200 nm. Sixteen scans were performed for each sample and the scans averaged.

Differential Scanning Calorimetry

Differential scanning calorimetry (DSC) was performed using a MicroCal Inc. VP DSC (MicroCal, Northampton, MA, USA) to determine the stability of rBoNTB(Hc) toward thermal unfolding under various pH and ionic strength conditions, by monitoring the unfolding transition temperature (T_m) and the unfolding transition enthalpy (ΔH). Scanning was performed from 5°C to 90°C at a scan rate of 1°C/min. All scans were performed twice to investigate reversibility of thermal unfolding. Analysis of the thermograms was performed using MicroCal Origin software.

Spectroscopy

Spectroscopy was performed using a Hewlett-Packard UV-visible spectrophotometer model 8453 (Palo Alto, CA) to quantify protein and to monitor aggregation. Concentration was evaluated by measuring absorbance at 280-nm wavelength and using an extinction coefficient of 1.94. Formation of insoluble aggregate matter, or denaturation was monitored by measuring absorbance at 360-nm wavelength.

Solubility

Studies investigating the effect of pH and NaCl on solubility of rBoNTB(Hc) were performed by using ultrafiltration techniques. To do this, the protein was dialyzed into the desired buffer of selected composition and pH, using the dialysis method described above, then placed in concentrators and concentrated by centrifugation. The concentration at the solubility limit was determined by UV spectroscopy as described above, after filtering the material through a 0.2-μm filter to remove precipitated protein.

SDS-PAGE

Nonreduced and reduced sodium dodecyl sulfate-poly acrylamide gel electrophoresis (SDS-PAGE) gels were used to qualitatively assess aggregation or breakdown of rBoNTB(Hc). Reduced gels were prepared by using preparation buffer containing 2-mercaptoethanol. All samples were heated at 95°C prior to loading onto the gel. Forty microliters of each sample was loaded onto a 4–20% Tris-glycine gradient gel. Gels were run at 35 mA for 1 h and subsequently stained overnight in colloidal Coomassie blue.

Size Exclusion Chromatography with On-line Light Scattering and Refractive Index Detectors

Size exclusion chromatography (SEC) was used to qualitatively monitor aggregation and breakdown of rBoNTB(Hc). A TosoHaas G300SW$_{xl}$ 7.8 × 300 mm, 5-μm column was used (Pharmacia Biotech, Piscataway, NJ, USA) with a Hewlett Packard model 1100 high performance liquid chromatography (HPLC) system. The mobile phase was 10 mM sodium phosphate with 150 mM sodium chloride, pH 7.4, at a flow rate of 0.5 ml/min. Detection of the eluting compounds was measured at 280-nm wavelength.

The light scattering detector was a Dawn DSP equipped with multiangle light scattering detectors, and the refractive index detector was an Optilab DSP (Wyatt Technology Corporation, Santa Barbara, CA, USA). A dn/dc of 0.185 ml/g was used. This is the change in refractive index with concentration and is practically independent of amino acid composition. Because the extinction coefficient of the protein is known, the UV detector was used to characterize the protein. The calibration constant for the UV detector was calculated as follows:

$$(\mathrm{dn/dc} \times \text{UV detector response factor}) / (\varepsilon^{\mathrm{g/ml}} \times \text{UV cell path length})$$

The basic light scattering equation is:

$$K^*c/R_\theta = 1/M_w[1 + 16\pi^2/3\lambda^2 \langle r_g^2 \rangle \sin^2(\theta/2)]$$

M_w is calculated using the Debye plot, which is a plot of K^*c/R_θ vs. $\sin^2(\theta/2)$

The intercept with the y axis (K^*c/R_θ) gives the reciprocal of molecular weight.

$$K^* \text{ is an optical parameter} = 4\pi^2(\mathrm{dn/dc})^2 n_o N_A \lambda_o^{-4}.$$

where n_o is the refractive index of the solvent, r_g^2 is the mean square radius of the solute, N_A is Avogadro's number, λ_o is the vacuum wavelength of the incident light, c is the concentration of the solute molecules, and R_θ is the excess intensity of light scattered at angle θ (i.e., the intensity due to the solute).

Hydrophobic Interaction Chromatography-HPLC

A TosoHaas SP-5PW 7.5 mm × 7.5 cm column was used (Pharmacia Biotech) with a Hewlett Packard model 1100 HPLC system to evaluate chemical and conformational stability of rBoNTB(Hc). Mobile phase A consisted of 50 mM sodium phosphate and 1.5 M ammonium sulfate, pH 6.8. Mobile phase B was 50 mM sodium phosphate, pH 6.8. Flow rate was set at 0.5 ml/min, with a 35-min run time. A gradient method was used with mobile phase B at 10% initially for 3 min, with a ramp to 77% by 10 min, another ramp to 89% mobile phase B by 30 min, and 100% mobile phase B by 31 min. Mobile phase B is again decreased to 10% by 33 min into the run. Detection of eluting components was measured at 210 nm with reference wavelength of 360 nm.

Peptide Mapping

Peptide mapping was performed to asses chemical changes occurring in high pH rBoNTB(Hc) formulations. Samples were diluted with 50 mM phosphate buffer, pH 7.5 (1:1v/v), and Endoproteinase Lys-C was added to a concentration of 150 mAu enzyme/mg of protein. The samples were incubated for 4 h at 37°C, and the digestion was stopped by the addition of 10% TFA. A Vydac C18, 2.0 × 250 mm, 5-mm

column (Grace Vydac, Hesperia, CA) was used for reverse phase separation with 0.1% TFA in water used as mobile phase A and 0.1% TFA in acetonitrile used as mobile phase B. The percentage of B was changed from 0.5% to 50% over 80 min and increased to 90% by 90 min during the separation. On-line mass spectrometric data was obtained using a LCQ classic instrument.

RESULTS

Solubility Studies

Solubility of rBoNTB(Hc) is extremely dependent on both pH and ionic strength as indicated by Fig. 1. The pH of minimum solubility in the absence of NaCl as would be expected is at the pI, between pH 6 and 7.5. Ionic strength is seen to have a significant effect on the rBoNTB(Hc) solubility profile as seen in Fig. 1. The presence of 150 mM NaCl shifts the pH of minimum solubility to higher pH values. The shift in the pH-solubility relationship suggests a possible interaction of cations with the negatively charged rBoNTB(Hc) molecule, perhaps resulting in a masking of electrostatic charges and an increase of the apparent isoelectric pH.

Differential Scanning Calorimetry

Figure 2a shows the effect of pH and NaCl on the unfolding transition temperature T_m. Figure 2b shows the effect of pH and NaCl on the enthalpy (ΔH) of the unfolding transition. T_m is highest at pH 4.0 and decreases almost linearly as pH increases above 5. At low pH, NaCl slightly increases the T_m. At pH of 7.5 and greater, the addition of NaCl leads to a decrease in T_m, with the decrease being very significant at pH 9. Minimal change in ΔH is seen between pH 4 and 7.5. Above pH 7.5, a distinct decrease in ΔH is observed. Deconvoluted unfolding transitions of rBoNTB(Hc) at pH 4, pH 9 with 150 mM NaCl and pH 9 without NaCl are presented in Figs. 3a–3c. The unfolding transitions at pH 4–7.5 with and without NaCl were identical. The unfolding transitions at pH 8 and 9 were also very similar to each other, but different from the transitions at pH 4–7.5. NaCl has a significant effect on the unfolding transition at pH 8 and 9.

Circular Dichroism

CD studies indicate that rBoNTB(Hc) consists predominantly of β-sheets. The classical pattern typical of β-sheet structures with a single minimum at 216–218-nm wavelength (22–24) is observed. Similarly to the DSC results, the CD spectra are identical between pH 4 and 7.5 but differ from the spectra of rBoNTB(Hc) at pH 8 and 9 (Fig. 4). At pH 8 and 9, a reduction in the positive peak at 230 nm and the negative peak at 216 nm were observed. No effect of NaCl was observed at high pH. A slight loss of ellipticity at 216 nm was also observed at pH 4 in the presence of NaCl. Conformation of rBoNTB(Hc) at high pH was shown to change with time (unfolding occurred) contrary to the effect observed at low pH (Fig. 5).

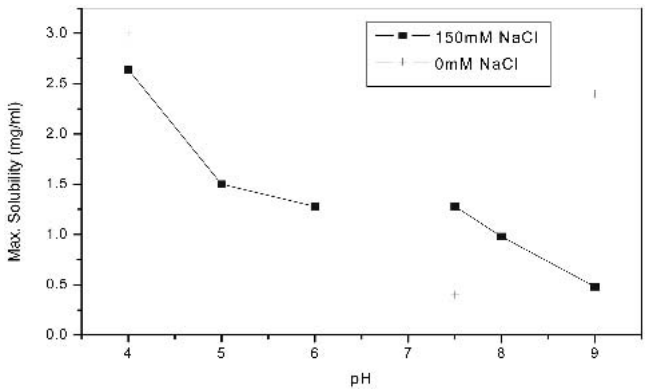

Fig. 1. Plot of maximum solubility of BoNTB(Hc) vs. pH.

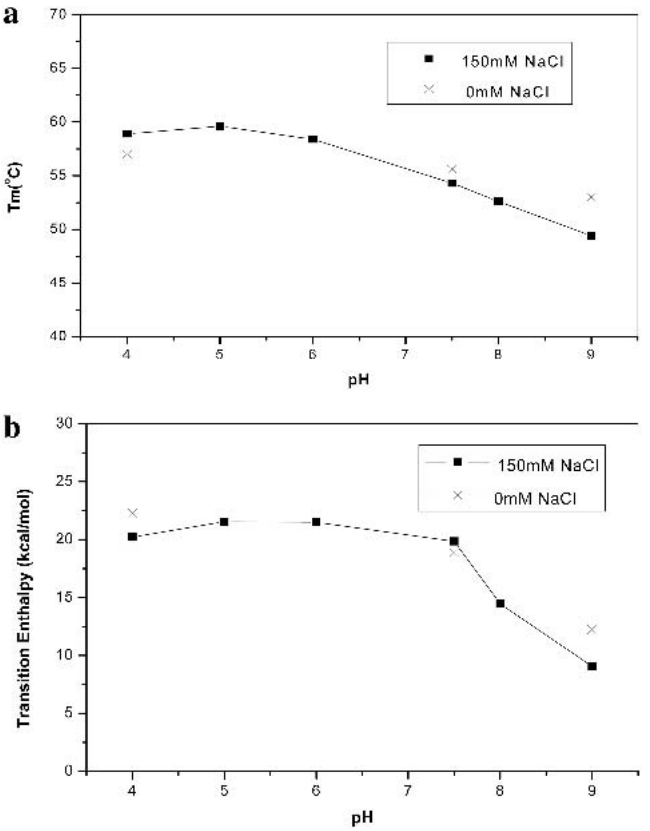

Fig. 2. (a) Plot of unfolding transition temperature of BoNTB(Hc) Tm vs. pH. (b) Plot of unfolding transition enthalpy of BoNTB(Hc) ΔH vs. pH.

Spectroscopy

The results of a 1-week stability study at 30°C evaluating the effect of pH and NaCl on aggregation and protein loss are shown in Table I. Analysis indicates minimal protein loss between pH 4 and 6, with or without NaCl after 1 week at 30°C. Formulations at pH 8 and 9 also showed no protein loss in the absence of NaCl. Formation of insoluble aggregates was observed at pH 7.5 with and without NaCl and at pH 9 in the presence of NaCl.

SDS-PAGE

The results of SDS-PAGE at time zero and after 1 week at 30°C are presented in Fig. 6. A single band indicating a homogenous population of monomeric rBoNTB(Hc) is observed at time zero for formulations at pH 4–6. Time zero formulations at pH 7.5–9.0 already show the presence of higher molecular weight compounds in nonreduced gels but are not observed in the reduced gels (Figs. 6a and 6b). After 1 week at 30°C, a single band at 50 kDa is still observed for pH 4–6 formulations. At pH 7.5 and higher, the rBoNTB(Hc)

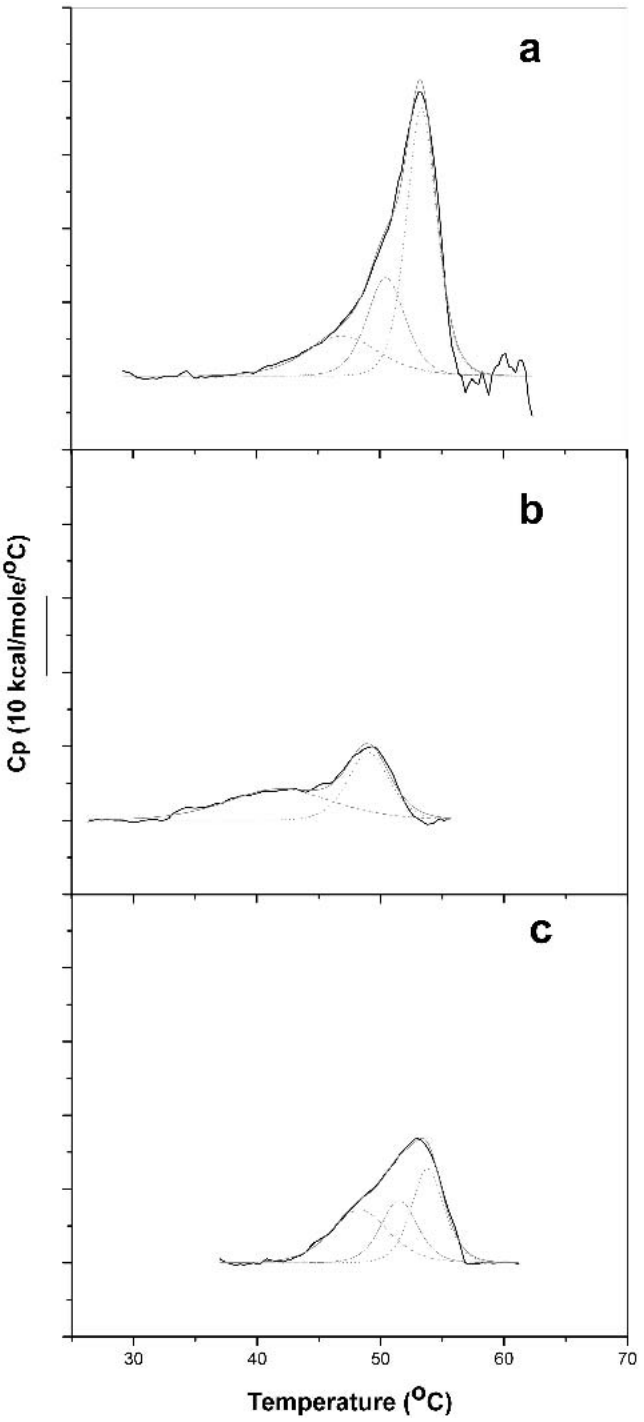

Fig. 3. Deconvolution of the unfolding transitions of BoNTB(Hc). (a) Unfolding transition between pH 4 and 7.5; (b) unfolding transition at pH 8 and 9 with 150 mM NaCl; (c) unfolding transition at pH 8 and 9 without NaCl. The solid lines represent the overall unfolding transitions obtained from the DSC scan, whereas the dotted lines are results of the deconvolution representing separate theoretical unfolding domains.

monomer bands exist as doublets. Several higher molecular weight bands are also observed in the nonreduced gels (Fig. 6c).

Hydrophobic Interaction Chromatography-HPLC

The results of analysis by hydrophobic interaction chromatography (HIC)-HPLC are presented in Fig. 7. For pH 4–6

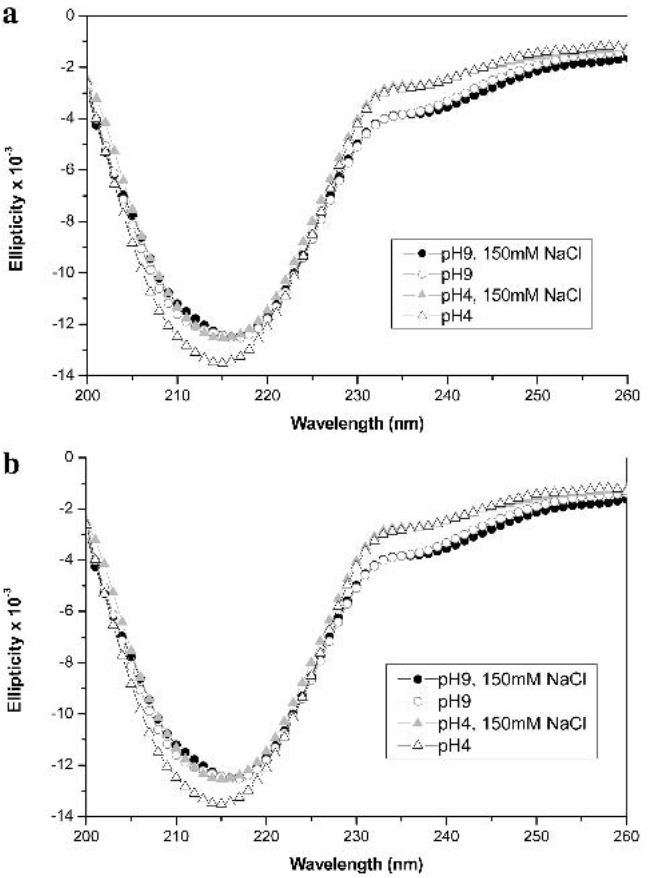

Fig. 4. (a) Effect of pH on secondary structure of BoNTB(Hc) by CD. (b) Effect of NaCl on secondary structure of BoNTB(Hc) by CD.

formulations at T = 0, a single peak is obtained with retention time 26.5 min, characteristic of rBoNTB(Hc). At pH 7.5 with and without NaCl , two peaks are obtained with retention times of 25.0 and 26.5 min. The 25.0-min peak exists as a shoulder. For formulations at pH 8–9, a retention time of 25 min with a small shoulder at 23.5 min is observed. After 1 week at 30°C, a single peak was still observed for pH 4–6 conditions with the same retention time of 26.5 min. The

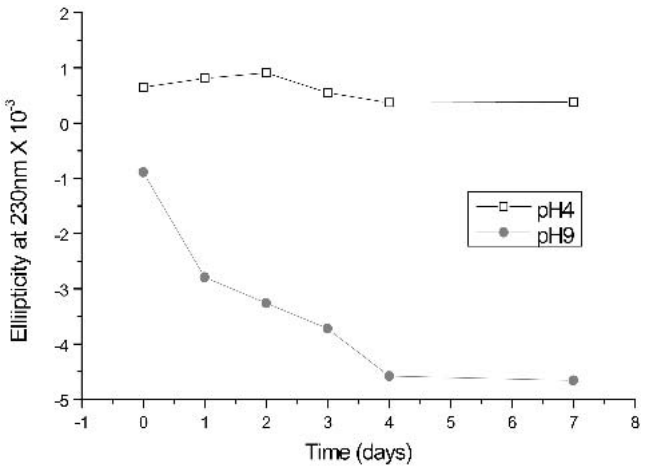

Fig. 5. Effect of time on unfolding of rBoNTB(Hc) at high and low pH by evaluating ellipticity at 230 nm by CD.

Table I. Effect of pH on Stability of BoNTB(Hc)

	Initial A_{360}	Initial conc. A_{280}	Final* A_{360}	Final* A_{360} filtered 0.2 μm	Final* conc. A_{280} filtered
pH 4	0.004	0.20	0.004	0.004	0.20
pH 4, NaCl†	0.001	0.20	0.062	0.001	0.19
pH 5	0.000	0.20	0.016	0.001	0.18
pH 6	0.000	0.20	0.017	0.002	0.19
pH 7.5	0.000	0.20	0.615	0.002	0.10
pH 7.5, NaCl†	0.000	0.20	0.404	0.001	0.13
pH 8	0.004	0.20	0.033	0.005	0.20
pH 9	0.000	0.20	0.028	0.004	0.20
pH 9, NaCl†	0.002	0.20	0.849	0.001	0.03

* One week storage at 30°C.
† NaCl refers to 150 mM NaCl.

double peak was again observed at pH 7.5; however, the area of the 25-min peak was significantly reduced. For the pH 8 and 9 conditions, no recovery of the protein was obtained after storage for 1 week at 30°C. The buffer peak is observed at approximately 5.5.min.

SEC-HPLC

SEC was only performed on pH 4 and pH 9 formulations to complement SDS-PAGE studies. rBoNTB(Hc) elutes from the SEC column with an apparent molecular weight of 16 kDa. However, calculation of molecular weight using the Debye plot (not shown), as described in "Materials and Methods," confirms an eluting product of molecular weight 50 kDa. At time zero and after 1 week, a single peak with a retention time of 18.8 min was obtained for the pH 4 formulation. The pH 9 condition, however, provided evidence of a higher molecular weight fraction eluting with a broad band at approximately 10 min. Negligible recovery of rBoNTB(Hc) from the column occurred after 1 week at 30°C.

Peptide Mapping

The reverse phase chromatograms obtained by peptide mapping analysis of rBoNTB(Hc) formulated in 25 mM sodium acetate, pH 5, and rBoNTB(Hc) in Tris buffer, pH 10.0 (to further increase our ability to monitor deamidation), are shown in Figs. 8a and 8b, respectively. Lys-C cleaves proteins at the C-terminus of the lysine residues, and 43 peptides, L1 through L43, are therefore predicted to be formed with rBoNTB(Hc). These peptides are shown in Table II. As shown in Fig. 8a, all of the peptides >400 Da predicted for a Lys-C digestion, except L33, were identified in rBoNTB(Hc) digest. All four of the cysteine-containing peptides L9, L35, L38, and L42 were identified. However, a small peak corresponding to disulfide bonded peptide L38-42 was also observed in the digest of the reference standard at pH 7.5. In addition, a small peak corresponding to the deamidated peptide of L14 (* in Fig. 8a), which showed a 1 Da mass increase, was also identified. An increased amount of deamidation was observed at pH 10, with peaks corresponding to peptides L14 (*2), L22 (*1), and L16 (*3) being identified and their identity confirmed by mass spectrometric analysis (Fig. 8b). In addition, an increased amount of disulfide bonding was also observed at pH 10.0. Peptides L35 and L9 containing free cysteines (aa369 and aa103) showed slight decrease in intensity, while new peaks corresponding to disulfide bonded peptides L35-42 (S2, 56.4 min), L9-38 (S4, 58.9 min), and L9-35 (S3, 57.9min) appeared. The intensity of the disulfide bonded peptide L35-42 (S1, 53.0 min) also increased.

DISCUSSION

Solubility studies in the absence of NaCl provided expected results with rBoNTB(Hc) being least soluble (0.5 mg/ml) at the isoelectric pH (pI) of 6.5–7.5 and increasing in solubility as pH is increased or decreased beyond the pI. At pH 4.0 in the presence of NaCl, the protein solubility exceeded 2.5 mg/ml. As pH was increased above pH 7.5, solubility decreased steadily to 0.5 mg/ml at pH 9 (Fig. 1). Increased interactions between the increasingly negatively charged ions and cations as explained in the "Results" section could be the reason for this. Another possibility is an unfolding of the molecule as suggested by DSC and CD studies (Figs. 3–5) leading to the exposure of hydrophobic residues and thus decreased solubility. Solubility at pH 7.5 in the presence of 150 mM NaCl was 1.1 mg/ml probably due to a salting-in effect of the neutral molecule. The solubility study suggests that to avoid protein losses by precipitation, exposure of rBoNTB(Hc) to high pH, high ionic strength conditions should be avoided to maximize process yields.

An increase in the conformational stability of rBoNTB(Hc) was observed at low pH, leading to an increase in T_m by DSC analysis (Fig. 2a). Evaluation of ΔH, which is the energy input required to unfold the protein, supports this observation (Fig. 2b). The most significant increase in stability was observed as the pH was decreased below the pI of rBoNTB(Hc). Detailed analysis of the profiles of the DSC thermograms suggests that different conformations of the protein exist above and below a pH of 7.5 either in the presence or absence of NaCl. Calculation of the peak widths of the unfolding transitions at half peak height indicate a less cooperative unfolding transition at pH 8 and 9 (Fig. 3). The broader transitions suggest a more loosely packed protein structure above pH 7.5 resulting from some unfolding of the protein. Deconvolution of the DSC thermograms produces three theoretical unfolding domains for the protein at pH 7.5 and below, with and without NaCl. At pH 8 and 9, however, only two unfolding domains are observed in the presence of NaCl, whereas in the absence of NaCl three unfolding domains are observed. In the absence of NaCl, cooperativity of the unfolding transition increases (narrower unfolding transition), indicating a reduction in the extent of unfolding (Fig. 3).

CD analysis of rBoNTB(Hc) supports the inferences made from DSC analysis. The secondary structure of rBoNTB(Hc) was similar between pH 4 and 7.5 and differed at pH 8 and 9 (Fig. 4). The far UV spectrum of rBoNTB(Hc) is characterized by a small absorption with a maximum centered around 230 nm and a more intense negative peak centered around 216 nm. The positive peak at 230 nm has been suggested to originate from the aromatic contribution to the far UV spectrum (24). This has been observed in several small structurally characterized β-sheet structures (25). The reduction in both peaks at high pH suggests some unfolding of rBoNTB(Hc).

These conformational studies suggest that a process fa-

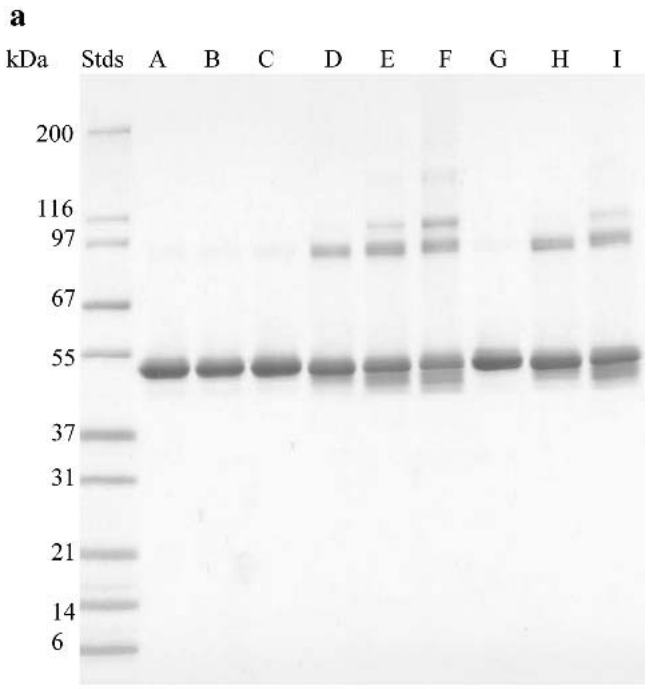

A - 10mM Acetate pH 4.0
B - 10mM Acetate pH 5.0
C - 10mM Citrate pH 6.0
D - 10mM Phosphate pH 7.5
E - 10mM Tris pH 8.0
F - 10mM Tris pH 9.0
G - 10mM Acetate, 150mM Sodium Chloride pH 4.0
H - 10mM Phosphate, 150mM Sodium Chloride pH 7.5
I - 10mM Tris, 150mM Sodium Chloride pH 9.0

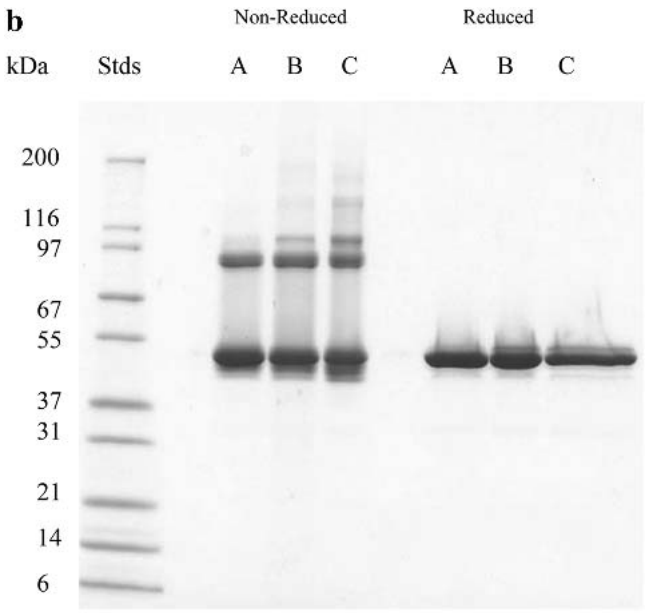

A - 10mM Phosphate pH 7.5
B - 10mM Tris pH 8.0
C - 10mM Tris pH 9.0

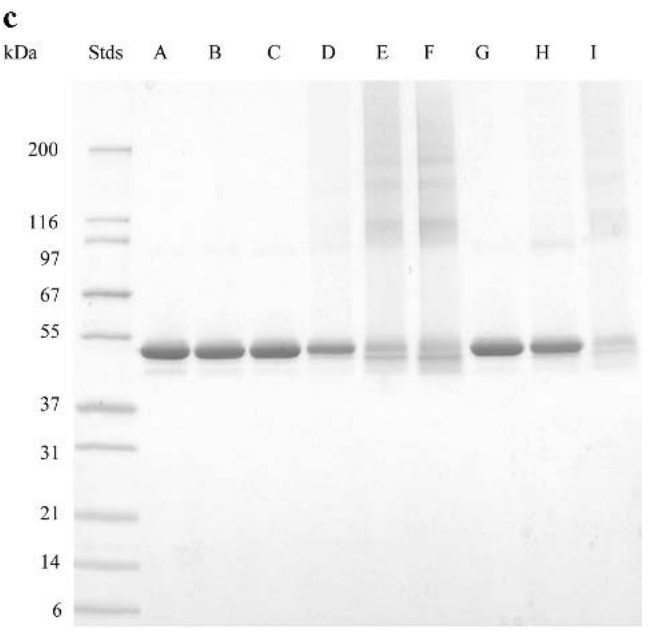

A - 10mM Acetate pH 4.0
B - 10mM Acetate pH 5.0
C - 10mM Citrate pH 6.0
D - 10mM Phosphate pH 7.5
E - 10mM Tris pH 8.0
F - 10mM Tris pH 9.0
G - 10mM Acetate, 150mM Sodium Chloride pH 4.0
H - 10mM Phosphate, 150mM Sodium Chloride pH 7.5
I - 10mM Tris, 150mM Sodium Chloride pH 9.0

Fig. 6. (a) Nonreduced SDS-PAGE gel of initial formulations of BoNTB(Hc) at varying pH and NaCl concentrations. (b) Reduced and nonreduced SDS-PAGE gels of BoNTB(Hc) at high pH. (c) Nonreduced SDS-PAGE gels of BoNTB(Hc) at varying pH and NaCl concentrations after storage for 1 week at 30°C.

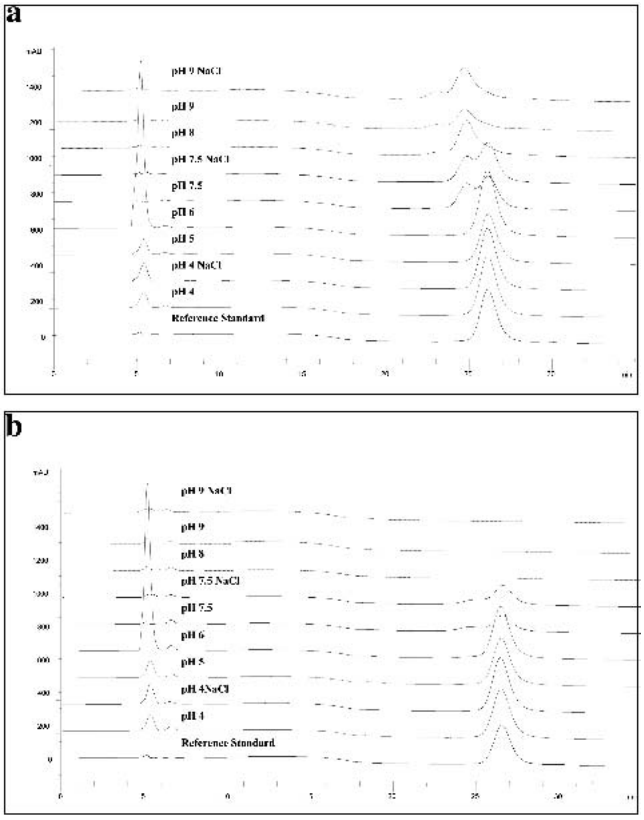

Fig. 7. (a) HIC-HPLC analysis of initial formulations of BoNTB(Hc) at varying pH and NaCl concentrations. (b) HIC-HPLC analysis of BoNTB(Hc) at varying pH and NaCl concentrations after storage for 1 week at 30°C.

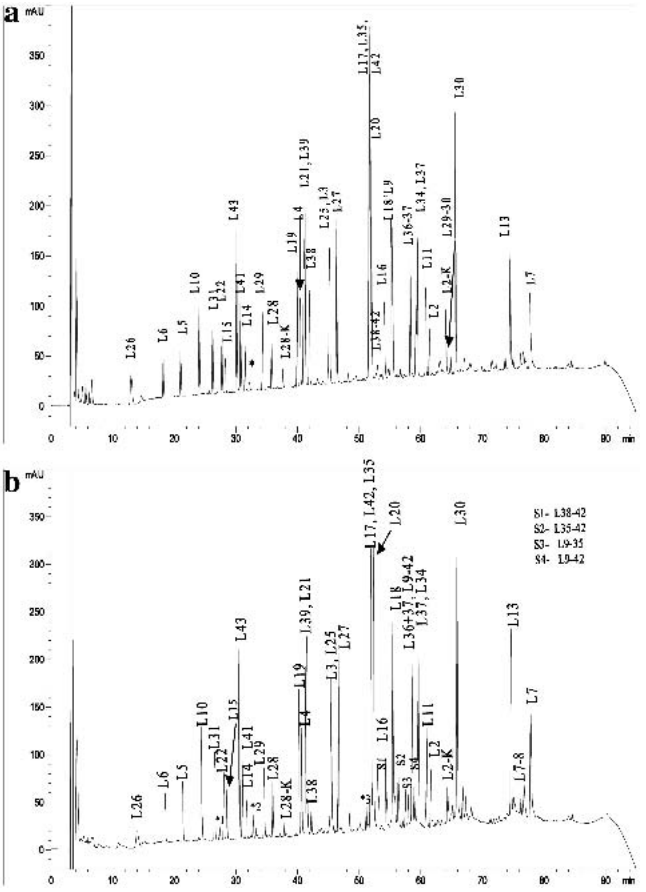

Fig. 8. (a) Peptide maps of rBoNTB(Hc) showing resulting peptides separated by reverse-phase HPLC chromatography. (b) Peptide maps of rBoNTB(Hc) formulated at pH 10.0 and stored at 30°C for 1 week.

voring low pH conditions will be effective in maintaining protein conformation. Exposure to high pH conditions, especially in the presence of high salt, should be minimized to maintain conformation of the protein in order to maintain stability and bioactivity. Very importantly, DSC studies also showed rBoNTB(Hc) unfolding under the evaluated conditions to be irreversible.

To further aid in understanding the effects of pH and NaCl on rBoNTB(Hc), a stability study was performed at pH 4, 5, 6, 7.5, 8, and 9, also pH 4, 7.5, and 9 with 150 mM NaCl. All formulations were stored at 30°C for 1 week and analyzed by SDS-PAGE, SEC-HPLC, UV_{280}, UV_{360}, HIC-HPLC, and CD. All formulations were filtered and diluted to a concentration 0.2 mg/ml of rBoNTB(Hc) prior to the start of the study. This concentration was selected in order to remain significantly below the solubility limits of the protein under the least soluble conditions (see solubility results). As shown in Table I, after 1 week at 30°C, extensive formation of insoluble particulate matter was obtained at pH 9, 150 mM NaCl, and only 0.03 mg/ml of protein remained in solution after filtration. Significant loss of material due to denaturation was also observed at pH 7.5 with and without NaCl. No denaturation was observed for rBoNTB(Hc) formulated at pH 4–6. A_{360} indicated the presence of minimal denaturation at pH 4.0 in 150 mM NaCl. Stability of rBoNTB(Hc) toward denaturation is therefore optimal at low pH; however, the presence of NaCl could increase the susceptibility of the protein toward aggregation.

SDS-PAGE results indicate that rBoNTB(Hc) forms disulfide bridges leading to the formation of higher molecular weight compounds at pH of 7.5 and above (Figs. 6a and 6b). These aggregates were observed in the T = 0 material and increased with an increase in pH above 7.5. Peptide map analysis confirmed disulfide bond formation at high pH. Intramolecular disulfide bonding in rBoNTB(Hc) monomers was responsible for the monomer doublet bands observed at pH 7.5 and higher. The SDS-PAGE gels were run under both nonreducing and reducing conditions. The higher molecular weight bands and also the doublet bands were absent in the reduced gels (Fig. 6b). This confirmed that the higher molecular weight compounds were formed as a result of intermolecular disulfide bond formation, and also some intramolecular bond formation led to the formation of doublets in the nonreduced gels. Optimal stability of the protein toward disulfide bond formation, and therefore formation of soluble aggregates, occurs between pH 4.0 and 6.0. No lower molecular weight products were observed in any formulation.

Separation of compounds by hydrophobic interaction chromatography is based on differences in extents of hydrophobic interaction between the various compounds and the column material leading to differences in retention time. A shift in retention time (RT) for rBoNTB(Hc) at pH 8 and 9 suggests some change in the electrostatic properties of rBoNTB(Hc) (Fig. 7a). The double peak observed at pH 7.5 indicates that a fraction of the material exhibits properties

Table II. Lys-Digested Peptides of rBoNTB(Hc)

Number		Average MW	Sequence
1	1-3	373.41	ANK
2	4-19	1980.29	YNSEILNNILNLRYK
3	20-32	1379.49	DNNLIDLSGYGAK
4	33-44	1379.49	VEVYDGVELNDK
5	45-48	535.60	NQFK
6	49-56	806.87	LTSSANSK
7	57-85	3530.13	IRVTQNQNIIFNSVLFDFFSV SWIRIPK
8	86-87	309.37	YK
9	88-106	2282.56	NDGIQNYIHNEYTIINCMK
10	107-112	704.74	NNSGWK
11	113-130	2082.48	ISIRGNRIIWTLIDINGK
12	131-132	247.29	TK
13	133-164	3958.40	SVFFEYNIREDISEYINRWFFV TITNNLNNAK
14	165-170	706.84	IYINGK
15	171-178	919.00	LESNTDIK
16	179-192	1616.88	DIREVIANGEIIFK
17	193-206	1738.00	LDGDIDRTQFIWMK
18	207-225	2368.58	YFSIFNTELSQSNIEERYK
19	226-234	1130.26	IQSYSEYLK
20	235-245	1384.58	DFWGNPLMYNK
21	246-255	1236.37	EYYMFNAGNK
22	256-260	623.71	NSYIK
23	261-262	259.35	LK
24	263-263	146.19	K
25	264-275	1301.46	DSPVGEILTRSK
26	276-281	752.78	YNQNSK
27	282-293	1546.74	YINYRDLYIGEK
28	294-299	832.06	FIIRRK
29	300-312	1475.58	SNSQSINDDIVRK
30	313-333	2820.11	EDYIYLDFFNLNQEWRVYTYK
31	334-336	456.54	YFK
32	337-337	146.19	K
33	338-341	533.54	EEEK
34	342-359	2067.32	LFLAPISDSDELYNTIQK
35	360-374	1863.05	EYDEQPTYSCQLLFK
36	375-375	146.19	K
37	376-402	3176.44	DEESTDEIGLIGIHRFYESGI VFEEYK
38	403-409	874.00	DYFCISK
39	410-413	608.74	WYLK
40	414-416	374.44	EVK
41	417-423	918.11	RKPYNLK
42	424-433	1204.44	LGCNWQFIPK
43	434-439	735.71	DEGWTE

similar to that of the high pH condition. No recovery of rBoNTB(Hc) was achieved at pH 8 and 9 by HIC-HPLC and also by SEC after 1 week at 30°C (Fig. 7b). A significant loss of the earlier eluting HIC peak at pH 7.5 also occurred after 1 week. A_{280}, however, indicates that there is minimal protein loss under these conditions in the absence of NaCl (Table I). Further investigation indicated that this lack of recovery at high pH after 1 week was due to rBoNTB(Hc) adsorption onto the column material. rBoNTB(Hc) could be recovered by running urea through the column.

In order to understand if the changes occurring in the protein at high pH resulting in such drastic changes in surface properties were due predominantly to chemical or structural changes, we proceeded to perform peptide mapping studies. Peptide mapping indicated that after exposing rBoNTB(Hc) to pH conditions as high as 10 for 1 week, at least 40–50% of the protein remained chemically unchanged, with the reminder forming disulfide bridges and undergoing deamidation (Fig. 8 and Table II). SDS-PAGE gels also show a significant fraction of the soluble monomer existing in solution initially and after 1 week in both pH 8 and 9 formulations (Fig. 6). Formation of dimers and oligomers are very unlikely to change the surface properties of the protein to such an extent.

In order to investigate structural changes with time, the pH 4 and pH 9 formulations were again prepared and stored at 30°C for 1 week. SEC and CD analysis were performed after 1, 2, 3, 4, and 8 days. The positive CD peak observed at 230 nm is measuring the asymmetry of aromatic side chain packing of the molecule (25–27). At T = 0, the ellipticity of the 230-nm peak for the pH 9 formulation is less than that of the pH 4 formulation. After 1 day at 30°C, the pH 9 formulation no longer exhibited a peak at 230 nm indicating a significant change in the asymmetry of the aromatic region of the protein after 1 day. Ellipticity at 230-nm wavelength continued to decrease with time until day 4. No further changes were observed between day 4 and day 8. This change in ellipticity was not observed with the pH 4 formulation. A plot of ellipticity at 230 nm vs. time is shown for both pH 4 and pH 9 formulations (Fig. 5). The SEC data is not shown; however, the structural changes observed by CD coincide with the loss in recovery of rBoNTB(Hc) from the SEC column. Significant reduction in recovery is observed for the pH 9 formulation at time zero compared to pH 4. After 1 day, recovery of the pH 9 formulation by SEC is minimal, and this corresponds to loss in asymmetry of the aromatic residues as determined by CD. By day 4, recovery is negligible, again corresponding to further loss in ellipticity at 230 nm.

This unfolding of the protein under high pH conditions, therefore, leads to the exposure of hydrophobic residues that alter the electrostatic properties of the molecular surface of rBoNTB(Hc) and lead to increased interaction with the HIC and SEC columns. Exposure to similar conditions should be minimized in our process to prevent loss of the product to columns and vessels.

This study provided us with a very good understanding of the effect of pH on the solubility, as well as physical and chemical stability of rBoNTB(Hc). Chemical and physical stability were found to be optimal at low pH. SDS-PAGE, HIC-HPLC, spectroscopy, and peptide map techniques aided in understanding the chemical and physical stability of rBoNTB(Hc) under the various pH conditions.

Long-term exposure to high pH conditions during the purification process will lead to decreases in product yields due to losses from covalent and noncovalent aggregation. Increased content of soluble impurities such as deamidated product would also be favored under the higher pH conditions. Conformational changes under the high pH conditions could also potentially negatively impact biological activity of the product. Biological activity of rBoNTB(Hc) has been shown to be dependent on conformation. The study suggests that any hold step during the process requires the protein to be stored under low pH conditions.

Information obtained by taking this approach of using biophysical studies in addition to the traditionally used analytical methods was very useful in understanding how various

conditions would affect the protein during the purification process and would subsequently help in the development of a robust purification process.

ACKNOWLEDGMENTS

This work was funded by DynPort Vaccine Company, LLC, and the Joint Vaccine Acquisition Program through the Department of Defense (contract no. DAMD17-98-C-8024).

REFERENCES

1. V. Sathyamoorthy and B. R. DasGupta. Separation, purification, partial characterization and comparison of the heavy and light chains of botulinum neurotoxin types A, B and E. *J. Biol. Chem.* **260**:10461–10466 (1985).
2. S. Bandyopadhyay, A. W. Clark, B. R. DasGupta, and V. Sathyamoorthy. Role of the heavy and light chains of botulinum neurotoxin in neuromuscular paralysis. *J. Biol. Chem.* **262**:2660–2663 (1987).
3. G. Schiavo, O. Rossetto, and C. Montecucco. Clostridial neurotoxins as tools to investigate the molecular events of neurotransmitter disease. *Cell. Biol.* **5**:221–229 (1994).
4. J. H. Anderson and G. E. Lewis. Clinical evaluation of botulinum toxoids. In G.E. Lewis (ed.), *Biomedical Aspects of Botulism*, Academic Press, New York, 1981, pp. 233–246.
5. L.A. Smith. Development of recombinant vaccines for botulinum neurotoxin. *Toxicon.* 1998; **36**:1539–1548 (1998).
6. D. Zabriskie. Strengthening the biological weapons convention and implications on the pharmaceutical and biotechnology industry. *Curr. Opin. Biotechnol.* **9**:312–318 (1998).
7. S. Swaminathan and S. Eswaramoorthy. Structural analysis of the catalytic and binding sites of Clostridium botulinum neurotoxin B. *Nat. Struct. Biol.* **7**:693–699 (2000).
8. L. L. Simpson. The origin, structure and pharmacological activity of botulinum toxin. *Pharmacol. Rev.* **33**:155–188 (1981).
9. B.R. DasGupta. The structure of botulinum neurotoxin. In L. L. Simpson (ed.), *Botulinum Neurotoxin and Tetanus Toxin*, Academic Press, New York, 1989, pp. 53–67.
10. L. L. Simpson. Peripheral actions of the botulinum toxins. In L. L. Simpson (ed.), *Botulinum Neurotoxin and Tetanus Toxin*, Academic Press, New York, 1989, pp. 153–178.
11. G. Schiavo, O. Rossetto, F. Benfenati, B. Poulain, and C. Montecucco. Tetanus and botulinum neurotoxins are zinc proteases specific for components of the neuroexocytosis apparatus. *Ann. N. Y. Acad. Sci.* **710**:65–75 (1994).
12. S. Bavari, D. D. Pless, E. R. Torres, F. J. Lebeda, and M. A. Olson. Identifying the principle protective antigenic determinants of type A botulinum neurotoxin. *Vaccine* **16**:1850–1856 (1999).
13. M. A. Clayton, J. M. Clayton, D. R. Brown, and J. L. Middlebrook. Protective vaccination with a recombinant fragment of Clostridium botulinum neurotoxin serotype A expressed from a synthetic gene in Escherichia coli. *Infect. Immunol.* **63**:2738–2742 (1998).
14. M. T. Dertzbaugh and M. W. West. Mapping of protective and cross-reactive domains of the type A neurotoxin of Clostridium botulinum. *Vaccine* **14**:1538–1544 (1996).
15. K. J. Potter, M. A. Bevins, E. V. Vassilieva, V. R. Chiruvolu, T. Smith, L. A. Smith, and M. M. Meagher. Production and purification of the heavy-chain fragment C of botulinum neurotoxin, Serotype B, expressed in the methylotrophic yeast pichia pastoris. *Protein Expr. Purif.* **13**:357–365 (1998).
16. M. P. Byrne, T. J. Smith, V. A. Montgomery, and L. A. Smith. Purification, potency and efficacy of the botulinum neurotoxin type A binding domain from pichia pastoris as a recombinant vaccine candidate. *Infect. Immunol.* **66**:4817–4822 (1998).
17. N. Kiyatkin, A. B. Maksymowych, and L. L. Simpson. Induction of an immune response by oral administration of recombinant botulinum toxin. *Infect. Immunol.* **65**:4586–4591 (1997).
18. H. F. LaPenotiere, M. A. Clayton, and J. L. Middlebrook. Expression of a large, nontoxic fragment of botulinum neurotoxin serotype A and its use as an immunogen. *Toxicon*. **33**:1383–1386 (1995).
19. M. C. W. Manning and R. Woody. Theoretical determination of the CD of proteins containing closely packed antiparallel β-sheets. *Biopolymers* **26**:1731–1752 (1987).
20. R. W. Woody. Circular Dichroism of peptides. In V. Hruby (ed.) *The Peptides, Analysis Synthesis and Biology*, Academic Press, New York, 1985, pp. 15–104.
21. W. Wang. Instability, stabilization and formulation of liquid protein pharmaceuticals. *Int. J. Pharm.* **185**:129–188 (1999).
22. F. Bedu-Addo, R. Moreadith, and S. J. Advant. Preformulation development of recombinant pegylated staphylokinase SY161 using statistical design. *AAPS Pharm. Sci.* **4**:19 1–11 (2002).
23. P. K. Tsai, D. B. Volkin, J. M. Dabora, K. C. Thompson, M. W. Bruner, J. U. Greiss, B. Matuszewska, M. Keogun, J. V. Bondi, and C. R. Middaugh. Formulation design of acidic fibroblast growth factor. *Pharm. Res.* **10**:649–659 (1993).
24. R. W. Woody. The circular dichroism of oriented β-sheets: Theoretical predictions. *Tetrahedron Asymmetry* **4**:529–544 (1993).
25. C. Krittanai and W. C. Johnson. Correcting the circular dichroism of peptides for contributions of absorbing side chains. *Anal. Biochem.* **253**:57–64 (1997).
26. R. W. Woody. Contribution of tryptophan side chains to the far-ultraviolet circular dichroism of proteins. *Eur. Biophys. J.* **23**: 253–262 (1994).
27. E. Koepf, H. M. Petrassi, M. Sudol, and J. W. Kelly. An isolated three-stranded antiparallel β-sheet domain that folds and refolds reversibly; evidence for a structured hydrophobic cluster in urea and GdnHCl and a disordered thermal unfolded state. *Protein Sci.* **8**:841–853 (1999).